AIP Advances

Gd(III) doping effect on magnetization and water proton relaxivities in ultra small iron oxide nanoparticles

Eun Sook Choi, Wenlong Xu, Myung Ju Baek, Ja Young Park, Joo Hyun Kim, Yongmin Chang, Tae Jeong Kim, and Gang Ho Lee

Citation: AIP Advances **3**, 072101 (2013); doi: 10.1063/1.4813307
View online: http://dx.doi.org/10.1063/1.4813307
View Table of Contents: http://scitation.aip.org/content/aip/journal/adva/3/7?ver=pdfcov
Published by the AIP Publishing

Gd(III) doping effect on magnetization and water proton relaxivities in ultra small iron oxide nanoparticles

Eun Sook Choi,[1] Wenlong Xu,[1] Myung Ju Baek,[2] Ja Young Park,[1]
Joo Hyun Kim,[3] Yongmin Chang,[2,3,a] Tae Jeong Kim,[2,4]
and Gang Ho Lee[1,2,a]
[1]*Department of Chemistry, College of Natural Sciences, Kyungpook National University, Taegu 702-701, South Korea*
[2]*Department of Nanoscience and Nanotechnology, Kyungpook National University, Taegu 702-701, South Korea*
[3]*Department of Molecular Medicine and Medical & Biological Engineering, School of Medicine, Kyungpook National University and Hospital, Taegu 702-701, South Korea*
[4]*Department of Applied Chemistry, College of Engineering, Kyungpook National University, Taegu 702-701, South Korea*

(Received 26 April 2013; accepted 24 June 2013; published online 2 July 2013)

Two samples of ultra small Gd(III) doped iron oxide nanoparticles were prepared to investigate Gd(III) doping effect on longitudinal (r_1) and transverse (r_2) water proton relaxivities. Gd(III) doping mole percents were 0.2 and 0.4 for samples 1 and 2, respectively. Average particle diameters were 2.5 to 2.1 nm for samples 1 and 2, respectively. Reduced r_1 and r_2 values were observed in both samples. We attributed this to reduced magnetizations arising from opposing effect of Gd(III) to net magnetizations of Fe(III)/Fe(II) in oxide nanoparticles. [http://dx.doi.org/10.1063/1.4813307]

I. INTRODUCTION

Magnetic properties of nanoparticles can depend on particle diameter because of anomalous surface spin effects related to unsaturated coordination of surface elements, surface oxidation, and surface coating.[1–4] Magnetic properties may also change with doping.

This work deals with Gd(III) doping in ultra small iron oxide nanoparticles. Note that Gd(III) has the largest 7 unpaired 4f electrons in the periodic table and thus, Gd(III) is regarded as the best element for T_1 MRI contrast agents because it strongly enhances the longitudinal water proton relaxation.[5,6] Furthermore, gadolinium oxide nanoparticles have shown r_1 values which are much larger than those of Gd(III)-chelates due to a dense population of Gd(III) ions in a nanoparticle.[7,8] Therefore, it is expected that Gd(III) doping might increase a longitudinal water proton relaxivity (r_1) in ultra small iron oxide nanoparticles (high spin doping effect). On the other hand, Gd(III) is known to oppose net magnetic moment of Fe(III)/Fe(II) in oxides, reducing magnetizations (reduced magnetization effect).[9–13] Such an opposing effect had been also observed in Fe thin films covered with Gd.[14–16] Therefore, these two effects will affect longitudinal (r_1) and transverse (r_2) water proton relaxivities, which was explored in this work.

In the previous work we developed ultra small iron oxide nanoparticles with an average particle diameter of 1.7 nm by refluxing Fe (III) precursor in triethylene glycol under air flow.[17] In this work we additionally doped tiny mole percents of Gd(III) into ultra small iron oxide nanoparticles. Core particle diameter, crystal structure, surface composition, surface coating, magnetic properties, r_1 and

[a]Corresponding authors: G. H. Lee: Tel.: -82-53-950-5340, Fax: -82-53-950-6330, E-mail address: ghlee@mail.knu.ac.kr; Y. Chang: Tel: -82-53-420-5471, E-mail address: ychang@knu.ac.kr

r_2 values, and map images were measured by using various techniques. Finally, Gd(III) doping effect on r_1 and r_2 values were investigated.

II. EXPERIMENTAL

A. Preparation

Two samples of ultra small Gd(III) doped iron oxide nanoparticles were prepared. In order to prepare sample 1, 0.1 mmol of $GdCl_3.xH_2O$, 10 mmol of $FeCl_36H_2O$, and 5 mmol of PEG diacid ($M_n = 600$) were added to 40 ml of triethylene glycol at room temperature. Reaction solution was magnetically stirred at 250 °C for 24 hours under air bubbling. In order to prepare sample 2, 1.0 mmol of $GdCl_3.xH_2O$ was used. The other reaction conditions were the same as the sample 1. After cooled to room temperature, product solutions were washed with 400 ml of distilled water twice. To do this, 400 ml of distilled water was added to the reaction solutions and then centrifuged. Top solutions were decanted and the remaining solutions were diluted with distilled water again for another washing. Halves of sample solutions were re-dispersed into distilled water for water proton relaxivity and map image measurements and the remaining samples were dried in air to obtain powder samples for various characterizations.

B. Characterization

Exact mole percents of Gd and Fe in nanoparticles were determined by using an inductively coupled plasma atomic emission spectrometer (ICPAES) (Thermo Jarrell Ash Co., IRIS/AP). In order to measure these, ~1 ml of each sample solution was pre-treated with 4 ml of HCl (or 3 ml of HCl and 1 ml of $HClO_4$) and then the solution was kept to 50–60 °C until nanoparticles were completely dissolved in solution. 2–3% HNO_3 solution was added to the above solution to dilute it. The final solution was weighed and then used for ICPAES measurement. The core particle diameters of PEG diacid coated ultra small Gd(III) doped iron oxide nanoparticles were measured by using a high resolution transmission electron microscope (HRTEM) (JEOL, JEM 2100F, 200 kV acceleration voltage). Nanoparticles dispersed in distilled water were dropped onto a 200-mesh copper grid covered with an amorphous carbon membrane by using a micropipette (Eppendorf, 2–20 μL), which was dried in air before loading into the microscope. A dynamic light scattering (DLS) particle size analyzer (UPA-150, Microtrac) was used to measure the hydrodynamic diameters of PEG diacid coated ultra small Gd(III) doped iron oxide nanoparticles dispersed in triply distilled water. The sample solution concentration used to measure hydrodynamic diameters was ~0.1 mM Fe. The crystal structure of powder samples was measured by using an X-ray diffraction (XRD) spectrometer (Philips, X-PERT PRO MRD). XRD patterns were recorded by using an unfiltered CuKα ($\lambda = 0.154184$ nm) radiation for $2\theta = 15$–90°. The surface coating of PEG diacid on nanoparticle surfaces was investigated by using a Fourier transform infrared (FT-IR) absorption spectrometer (Perkin Elmer, Spectrum GX & Auto Image) and a thermogravimetric analyzer (TGA) (TA Instruments, SDT-Q600). In order to record FT-IR absorption spectra, sample discs were prepared by pressing mixtures of KBr and powder samples. FT-IR absorption spectra were scanned between 400 and 4000 cm^{-1}. TGA curves were recorded to estimate the surface coating amounts and scanned between room temperature and 700 °C under air flow. The surface composition of Gd and Fe in nanoparticles was measured by using an X-ray photoelectron spectrometer (XPS) (ULVAC-PHI, Quantera SXM) with an Al Kα X-ray source (=1486.6 eV). Dried powder samples were loaded onto a carbon tape (5 × 5 mm) and XPS spectra were recorded between 0 and 1400 eV in electron binding energy (EBE) scale. A superconducting quantum interference device (SQUID) magnetometer (Quantum Design, MPMS-7) was used to study magnetic properties of ultra small Gd(III) doped iron oxide nanoparticles. Both magnetization (M) versus applied field (H) (i.e., M-H) curves ($-5 \leq H \leq 5$ tesla) at temperature (T) of 300 K and zero-field-cooled (ZFC) M-T curves ($5 \leq T \leq 330$ K) at H = 100 oersted (Oe) were recorded. Exactly weighed powder samples were loaded inside nonmagnetic gelatin capsules. Net magnetizations of ultra small Gd(III) doped iron oxide nanoparticles were obtained by using their net masses estimated from TGA curves. Both R_1

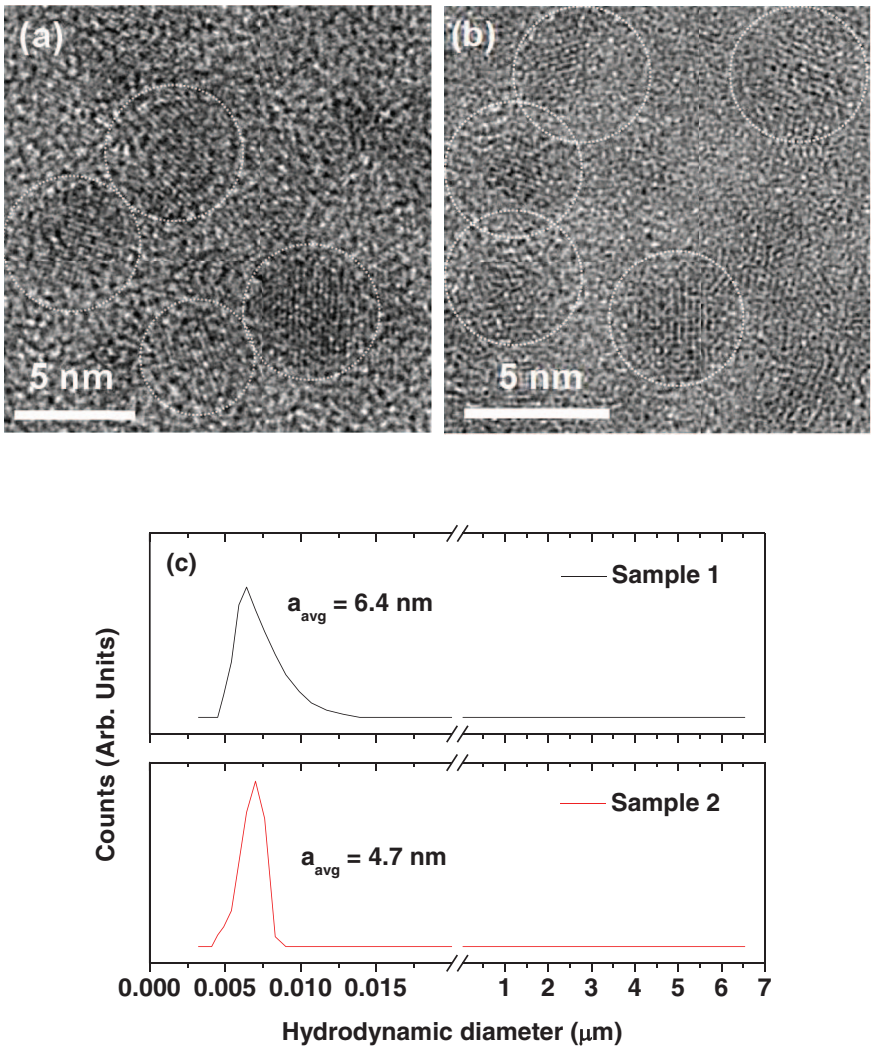

FIG. 1. HRTEM images ((a) sample 1 and (b) sample 2) and (c) DLS patterns of PEG diacid coated ultra small Gd(III) doped iron oxide nanoparticles. Dotted circles in HRTEM images indicate selected ultra small Gd(III) doped iron oxide nanoparticles.

and R_2 map images as well as both T_1 and T_2 relaxation times were measured by using a 1.5 tesla MRI instrument (GE medical system, GE 1.5 tesla Signa Advantage) equipped with the knee coil (EXTREM). A series of five aqueous sample solutions were prepared at different concentrations (1, 0.5, 0.25, 0.125 and 0.0625 mM Fe). Then, both map images and relaxation times were measured by using these solutions. r_1 and r_2 values were then estimated from the slopes in the plots of $1/T_1$ ($=R_1$) and $1/T_2$ ($=R_2$) as a function of Fe concentration, respectively. The measurement parameters used were as follows: the external MR field (H) = 1.5 tesla, the temperature = 22 °C, the number of acquisition (NEX) = 1, the field of view (FOV) = 16 cm, the phase FOV = 1, the matrix size = 512 × 512, the slice thickness = 5 mm, the spacing gap = 0, and the pixel bandwidth = 61.0547, the repetition time (TR) = 2009 ms, and the time to echo (TE) = 9 ms.

III. RESULTS AND DISCUSSION

A. Particle diameter, hydrodynamic diameter, and crystal structure

Figure 1 shows HRTEM images and DLS patterns of PEG diacid coated ultra small Gd(III) doped iron oxide nanoparticles. Average particle diameters (d_{avg}) of ultra small Gd(III) doped iron

TABLE I. Average particle diameter (d_{avg}), magnetization (M) at 5 tesla and 300 K, and water proton relaxivities (r_1 and r_2) at 1.5 tesla and 22 °C of various nanoparticles.

Sample	Ligand	d_{avg} (nm)	M (emu/g)	r_1 ($s^{-1}mM^{-1}$)	r_2 ($s^{-1}mM^{-1}$)	Ref.
Fe_3O_4/γ-Fe_2O_3	PEG diacid	1.7	6.5	4.46	15.01	17
Sample 1	PEG diacid	2.5	2.3	0.57	2.31	This work
Sample 2	PEG diacid	2.1	2.6	0.90	3.20	This work
Gd_2O_3	D-glucuronic acid	1.0	8.4	9.9	10.5	18

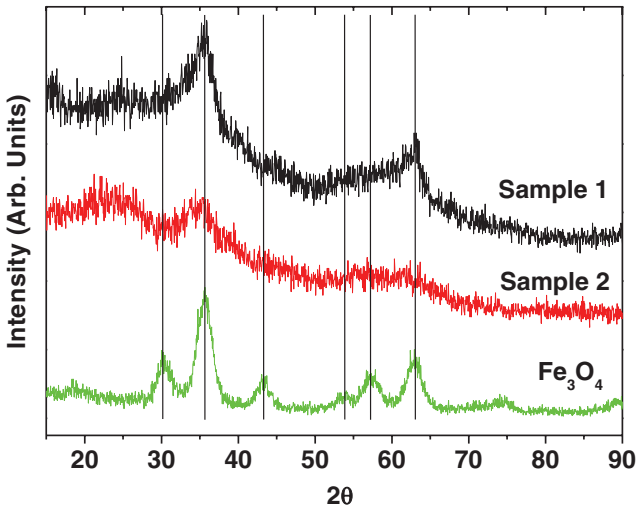

FIG. 2. XRD patterns of two powder samples of PEG diacid coated ultra small Gd(III) doped iron oxide nanoparticles. An XRD pattern of Fe_3O_4 nanoparticles was given as a reference.

oxide nanoparticles were estimated to be 2.5 and 2.1 nm for samples 1 and 2, respectively, and also provided in Table I. Average hydrodynamic diameters (a_{avg}) were estimated to be 6.4 and 4.7 nm for samples 1 and 2, respectively. XRD patterns indicated that the crystal structure of ultra small Gd(III) ion doped iron oxide nanoparticles closely corresponded to a face-centered cubic (fcc)[19] of Fe_3O_4 as shown in Figure 2. The broad peaks were likely due to ultra small particle diameters.[20]

B. Surface coating

Surface coating of ultra small Gd(III) doped iron oxide nanoparticles with PEG diacid was investigated by taking FT-IR absorption spectra as shown in Figure 3. Functional groups of PEG diacid such as the C=O stretch at 1590 and 1720 cm^{-1} and the C-H stretch at 2890 cm^{-1} confirmed the surface coating of ultra small Gd(III) doped iron oxide nanoparticles with PEG diacid. The PEG diacid has two -COOH groups per molecule. The stretch at 1590 cm^{-1} is due to –COOH conjugated to a nanoparticle whereas that at 1720 cm^{-1} is due to free, i.e., unconjugated –COOH. Red shift by $\sim$130 cm^{-1} in conjugated -COOH had been also observed in various metal oxide nanoparticles,[21–24] supporting our result. The weight percents of surface coated PEG diacid were estimated to be 53 and 66% for samples 1 and 2, respectively, from TGA curves as shown in Figure 4. These indicate that ultra small Gd(III) doped iron oxide nanoparticles were sufficiently coated with PEG diacid, which is necessary for water solubility. The remaining weight percents, i.e., 47 and 34% corresponded to net masses of ultra small Gd(III) doped iron oxide nanoparticles in samples 1 and 2, respectively.

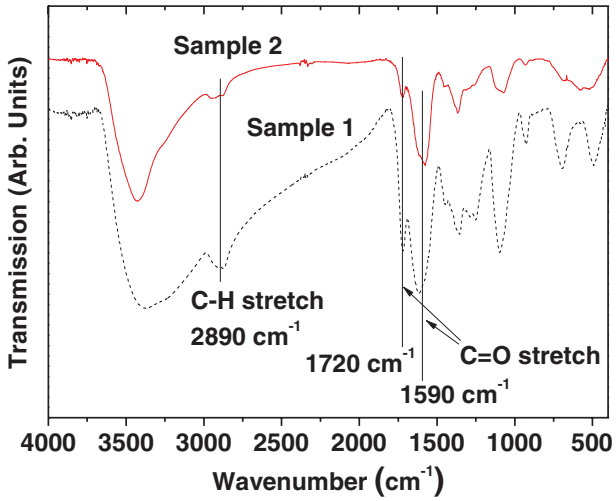

FIG. 3. FT-IR absorption spectra of two powder samples of PEG diacid coated ultra small Gd(III) doped iron oxide nanoparticles.

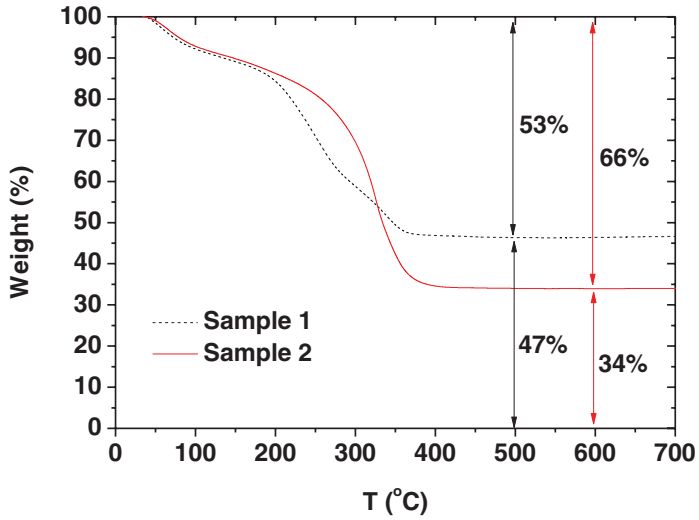

FIG. 4. TGA curves of two powder samples of PEG diacid coated ultra small Gd(III) doped iron oxide nanoparticles. The top and bottom values indicate weight percents of surface coated PEG diacid and ultra small Gd(III) doped iron oxide nanoparticles in powder samples, respectively.

C. Doping mole percent and surface composition in nanoparticles

Note that Gd(III) precursor mole percents used with respect to those of Fe(III) precursor in reaction were 1 and 10% for samples 1 and 2, respectively, as described in experimental section. However, Gd(III) doping mole percents in nanoparticles estimated from ICPAES analysis were 0.2 and 0.4% for samples 1 and 2, respectively. We attributed this large difference between precursor and doped Gd(III) mole percents as due to mismatch in ionic radius (i.e., a(Fe(III))/a(Gd(III)) = 0.58–0.74).[25] However, stoichiometric $Gd_xFe_yO_z$ oxides such as $GdFeO_3$, $GdFe_2O_4$, Gd_3FeO_6, and $Gd_3Fe_5O_{12}$ had been prepared at high temperature syntheses through annealing (>500 °C).[10,11,26–38] Therefore, high temperature synthesis should be used to increase Gd(III) doping mole percents.

XPS spectra were taken to investigate surface composition in nanoparticles as shown in Figure 5. As expected from ICPAES analysis, no or negligible signals from Gd (4d) were observed at 143.8 eV[39] within an experimental error limit whereas prominent signals from Fe ($2p_{3/2}$ and $2p_{1/2}$) were observed at 710.9 and 724.5 eV,[39] respectively, in both samples.

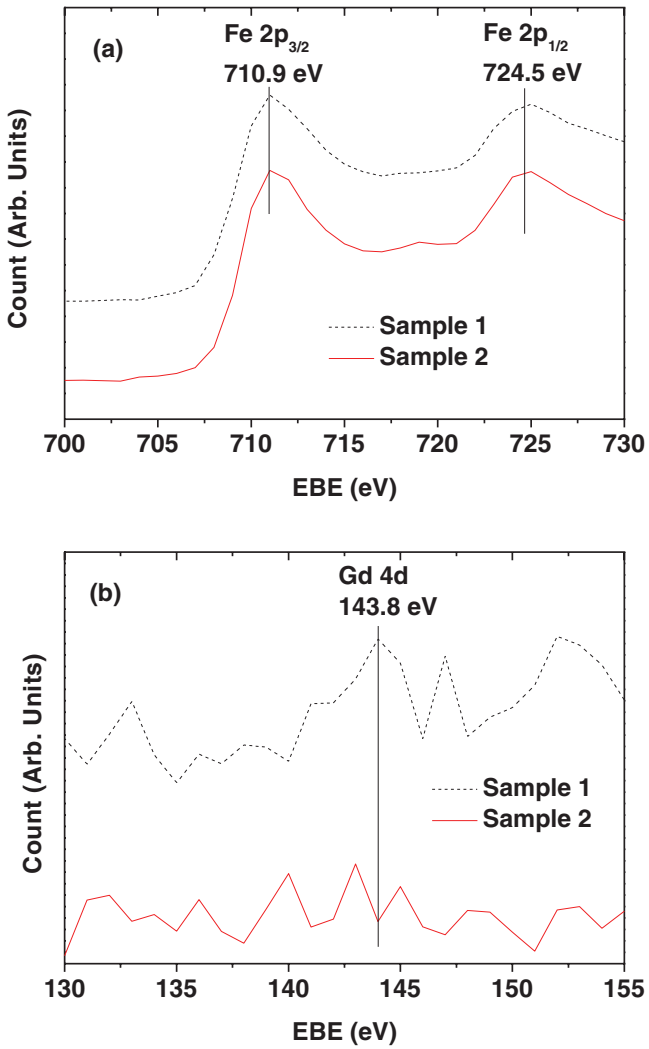

FIG. 5. XPS spectra of two powder samples of PEG diacid coated ultra small Gd(III) doped iron oxide nanoparticles: (a) Fe ($2p_{3/2}$ and $2p_{1/2}$) and (b) Gd (4d).

D. Magnetic properties

Magnetic properties were investigated by recording both M–H curves at T = 300 K and ZFC M–T curves at H = 100 Oe. Net magnetizations of ultra small Gd(III) doped iron oxide nanoparticles were obtained by using net masses of ultra small Gd(III) doped iron oxide nanoparticles in samples estimated from TGA curves. M-H and ZFC M-T curves are shown in Figures 6(a) and 6(b), respectively. Net magnetizations estimated at H = 5 tesla are provided in Table I. These magnetizations are smaller than that (=84 emu/g)[40] of bulk Fe_3O_4 because M–H curves were not fully saturated. An unsaturated M-H curve similar to ours was also observed for the spinel iron oxide nanoparticles with a mean particle diameter of 2.06 nm at room temperature by Yaacob *et al.*[41] They attributed this to a magnetically anomalous surface layer.

Carpenter suggested that the slope at the near zero field in a M–H curve for superparamagnetic nanoparticles with a size distribution should come from the largest nanoparticle.[42] He suggested that $d_{mag} = (18kT(dM/dH)_{H=0} / \pi\rho M_s)^{1/3}$ in which the d_{mag} is the maximum magnetic diameter, k the Boltzmann constant (=1.381 × 10^{-16} erg/K), T the temperature (=300 K), ρ the density of nanoparticles (g/cm^3), and $(dM/dH)_{H=0}$ the slope near the zero field. By using the estimated $(dM/dH)_{H=0}$ of 9.13617 × 10^{-5} and 5.6106 × 10^{-5} emu/gOe for samples 1 and 2, respectively, the saturation magnetization of 84 emu/g for bulk Fe_3O_4,[40] and the ρ (=5.1 g/cm^3) of bulk material

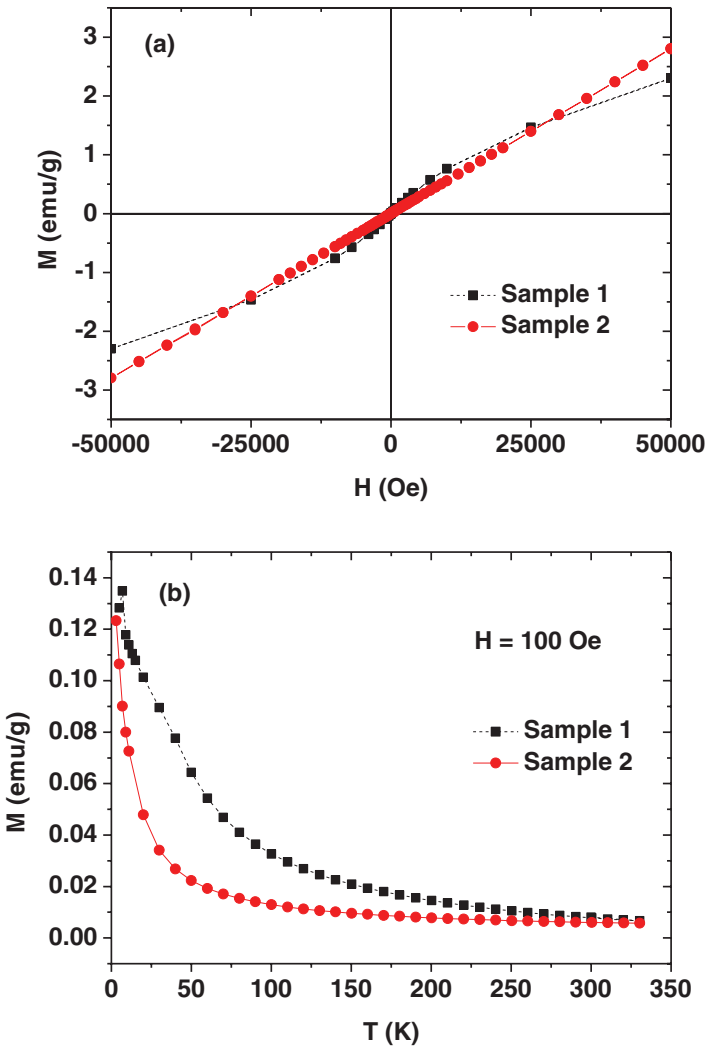

FIG. 6. (a) M-H curves at T = 300 K and (b) ZFC M-T curves at H = 100 Oe of two powder samples of PEG diacid coated ultra small Gd(III) doped iron oxide nanoparticles. M corresponds to net M of ultra small Gd(III) doped iron oxide nanoparticles in powder samples.

of Fe_3O_4,[43] the d_{mag} values were estimated to be 3.6 and 3.1 nm for samples 1 and 2, respectively. These values are slightly larger than average particle diameters of 2.5 and 2.1 nm estimated from HRTEM images, respectively. These are consistent with expectations because the d_{mag} corresponds to the largest nanoparticle in a size distribution.

As provided in Table I, net magnetizations in both samples were smaller than 6.5 and 8.4 emu/g of ultra small iron oxide nanoparticles[17] and ultra small gadolinium oxide nanoparticles,[18] respectively. Therefore, magnetization was reduced by doping Gd(III) into ultra small iron oxide nanoparticles. Reduced magnetizations in various Gd(III) substituted iron oxides had been also observed,[9–13] supporting our result. It was suggested in those works that Gd(III) opposed the net magnetic moment of Fe(III)/Fe(II) in oxides. An antiferromagnetic coupling between Gd and Fe in metallic thin films had been also reported,[14–16] supporting our result.

E. Water proton relaxivity and map image

Figure 7 shows plots of $1/T_1$ (=R_1) and $1/T_2$ (=R_2) inverse relaxation times (=relaxation rates) as a function of Fe concentration. The slops correspond to r_1 and r_2 relaxivities, respectively.

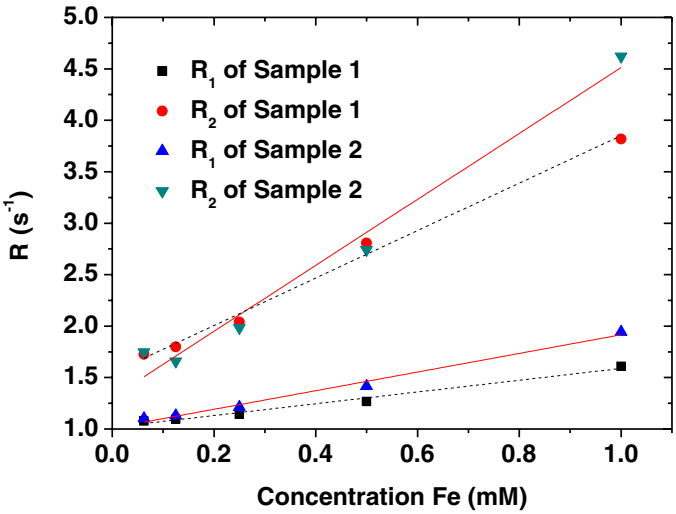

FIG. 7. Plots of R_1 ($=1/T_1$) and R_2 ($=1/T_2$) relaxation rates as a function of Fe concentration of two aqueous solution samples of PEG diacid coated ultra small Gd(III) doped iron oxide nanoparticles. The slopes correspond to r_1 and r_2 relaxivities, respectively.

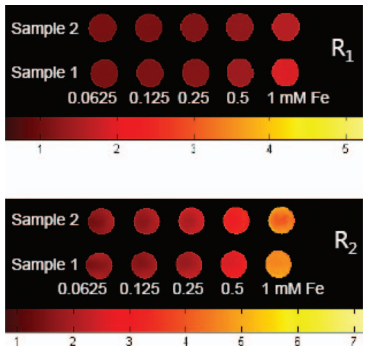

FIG. 8. R_1 and R_2 map images of aqueous sample solutions of PEG diacid coated ultra small Gd(III) doped iron oxide nanoparticles as a function of Fe concentration.

Table I lists relaxivities of various nanoparticles including PEG diacid coated ultra small Gd(III) doped iron oxide nanoparticles. R_1 and R_2 map images are presented in Figure 8. As expected from r_1 and r_2 values, dose-dependent contrast enhancements in R_1 map images were negligible and those in R_2 map images were only decent, implying that PEG diacid coated ultra small Gd(III) doped iron oxide nanoparticles are not suitable for both T_1 and T_2 MRI contrast agents at clinical MR fields.

Figure 9 clearly shows Gd(III) doping effect on magnetization and r_1 and r_2 values. That is, magnetizations and r_1 and r_2 values of two samples are smaller than those of ultra small iron oxide nanoparticles[17] and ultra small gadolinium oxide nanoparticles.[18] As investigated by others, magnetic moment of Gd(III) is anti-parallel to net magnetic moment of Fe(III)/Fe(II) in oxides.[9–13] Therefore, reduced magnetizations in both samples are due to this. Note that r_1 and r_2 values are proportional to square of magnetization.[44] Therefore, reduced r_1 and r_2 values are due to reduced magnetizations in both samples.

IV. CONCLUSIONS

In summary we for the first time investigated Gd(III) doping effect on magnetization and water proton relaxivities by synthesizing two samples of ultra small Gd(III) doped iron oxide nanoparticles. Gd(III) doping mole percents were 0.2 and 0.4% for samples 1 and 2, respectively. Average particle

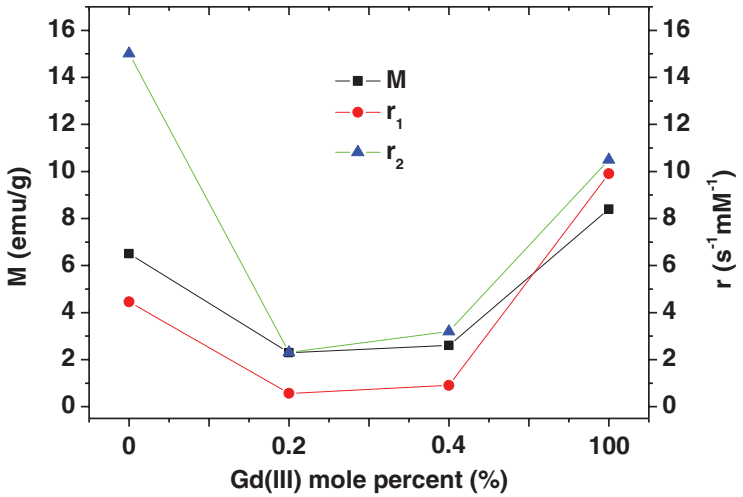

FIG. 9. Plots of magnetization (M) and water proton relaxivities (r_1 and r_2) of two samples of PEG diacid coated ultra small Gd(III) doped iron oxide nanoparticles as a function of Gd(III) mole percent.

diameters were 2.5 and 2.1 nm for samples 1 and 2, respectively. Although it was expected that doping of high spin Gd(III) (S = 7/2) into ultra small iron oxide nanoparticles would increase water proton relaxivities (especially, r_1 values), reduced r_1 and r_2 values were observed in both samples. This result was ascribed to opposing effect of Gd(III) on net magnetic moment of Fe(III)/Fe(II) in oxides, giving reduced magnetizations and as a result reduced r_1 and r_2 values.

ACKNOWLEDGMENTS

This work was supported by the Grant No. RTI04-01-01 from the Regional Technology Innovation Program of the Ministry of Commerce, Industry, and Energy funded by the Korean Government, the Korea Health Technology R&D Project, Ministry of Health & Welfare, Republic of Korea (A111345), the Basic Science Research Program through the National Research Foundation funded by the Ministry of Education, Science, and Technology (2011-0015353 to YC, 2013R1A1A4A03004511 to GHL, and 2010-0024143 to TJK), the R&D program of Ministry of Knowledgment Economy/Korea Evaluation Institute of Industrial Technology (10040393, development and commercialization of molecular diagnostic technologies for lung cancer through clinical validation), and Kyungpook National University Research Fund (2013). We thank the Korea Basic Science Institute for allowing us to use their HRTEM and XRD.

[1] D. L. Leslie-Pelecky and R. D. Rieke, Chem. Mater. **8**, 1770 (1996).
[2] Q. Li, C. M. Sorensen, K. J. Klabunde, and G. C. Hadjipanayis, Aerosol Sci. Technol. **19**, 453 (1993).
[3] D. Zhang, K. J. Labunde, C. M. Sorensen, and G. C. Hadjipanayis, Phys. Rev. B **58**, 14167 (1998).
[4] S. Gangopadhyay, G. C. Hadjipanayis, B. Dale, C. M. Sorensen, K. J. Klabunde, V. Papaefthymiou, and A. Kostikas, Phys. Rev. B **45**, 9778 (1992).
[5] P. Caravan, J. J. Ellison, T. J. McMurry, and R. B. Lauffer, Chem. Rev. **99**, 2293 (1999).
[6] R. B. Lauffer, Chem. Rev. **87**, 901 (1987).
[7] W. Xu, K. Kattel, J. Y. Park, Y. Chang, T. J. Kim, and G. H. Lee, Phys. Chem. Chem. Phys. **14**, 12687 (2012).
[8] T. J. Kim, K. S. Chae, Y. Chang, and G. H. Lee, Curr. Topic Med. Chem. **13**, 422 (2013).
[9] E. E. Anderson, J. R. Cunningham, Jr., and G. E. McDuffie, Phys. Rev. **116**, 624 (1959).
[10] R. M. Bozorth, H. J. Williams, and D. E. Walsh, Phys. Rev. **103**, 572 (1956).
[11] M. A. Gilleo, J. Chem. Phys. **24**, 1239 (1956).
[12] G. Litsardakis, I. Manolakis, and K. Efthimiadis, J. Alloy Comp. **427**, 194 (2007).
[13] R. N. Panda, J. C. Shih, and T. S. Chin, J. Magn. Magn. Mater. **257**, 79 (2003).
[14] C. Carbone, R. Rochow, L. Braicovich, R. Jungblut, T. Kachel, D. Tillmann, and E. Kisker, Phys. Rev. B **41**, 3866 (1990).
[15] K. J. H. Buschow, Rep. Progr. Phys. **40**, 1179 (1977).
[16] G. Panaccione, P. Torelli, G. Rossi, G. van der Laan, M. Sacchi, and F. Sirotti, Phys. Rev. B **58**, R5916 (1998).
[17] J. Y. Park, P. Daksha, G. H. Lee, S. Woo, and Y. Chang, Nanotechnology **19**, 365603 (2008).

[18] J. Y. Park, M. J. Baek, E. S. Choi, S. Woo, J. H. Kim, T. J. Kim, J. C. Jung, K. S. Chae, Y. Chang, and G. H. Lee, ACS Nano **3**, 3663 (2009).
[19] Card Number 19-0629, JCPDS International Center for Diffraction Data V. 1.30, 1997.
[20] B. D. Cullity, *Elements of X-Ray Diffraction* (Addison-Wesley, Reading, MA, 1978), p. 99.
[21] F. Söderlind, H. Pedersen, R. M. Petoral, Jr., P. O. Käll, and K. Uval, J. Colloids Interface Sci. **288**, 140 (2005).
[22] O. W. Duckworth and S. T. Martin, Geochim. Cosmochim. Acta **65**, 4289 (2001).
[23] S. J. Hug and D. Bahnemann, J. Electron Spectro. Relat. Phenomena **150**, 208 (2006).
[24] C. B. Mendive, T. Bredow, M. A. Blesa, and D. W. Bahnemann, Phys. Chem. Chem. Phys. **8**, 3232 (2006).
[25] J. A. Dean, *Lange's Handbook of Chemistry*, 14th. edition (McGraw Hill, New York, 1992), p. 4.14.
[26] S. Mathur, H. Shen, N. Lecerf, A. Kjekshus, H. Fjellvåg, and G. F. Goya, Adv. Mater. **14**, 1405 (2002).
[27] V. Bedekar, O. D. Jayakumar, J. Manjanna, and A. K. Tyagi, Mater. Lett. **62**, 3793 (2008).
[28] N. L. Ross, J. Zhao, and R. J. Angel, J. Solid State Chem. **177**, 3768 (2004).
[29] X. Niu, H. Li, and G. Liu, J. Mol. Cat. A: Chem. **232**, 89 (2005).
[30] M. Sivakumar, A. Gedanken, D. Bhattacharya, I. Brukental, Y. Yeshurun, W. Zhong, Y. W. Du, I. Felner, and I. Nowik, Chem. Mater. **16**, 3623 (2004).
[31] H. Xu, X. Hu, and L. Zhang, Crystal Growth Design **8**, 2061 (2008).
[32] D. H. Kuo and K. C. Huang, Ceram. Int. **34**, 1503 (2008).
[33] S. Musić, V. Ilakovac, M. Ristić, and S. Popović, J. Mater. Sci. **27**, 1011 (1992).
[34] F. Söderlind, M. A. Fortin, R. M. Petoral, Jr., A. Klasson, T. Veres, M. Engström, K. Uvdal, and P.-O. Käll, Nanotechnology **19**, 085608 (2008).
[35] S. C. Zanatta, L. F. Cótica, A. Paesano, Jr., S. N. de Medeiros, J. B. M. da Cunha, and B. Hallouche, J. Am. Ceram. Soc. **88**, 3316 (2005).
[36] M. H. Phan, M. B. Morales, C. N. Chinnasamy, B. Latha, V. G. Harris, and H. Srikanth, J. Phys. D: Appl. Phys. **42**, 115007 (2009).
[37] D. Rodic, J. Konstantinovic, and A. Szytuła, Solid State Comm. **58**, 111 (1986).
[38] A. N. Thakur, K. Gaur, and H. B. Lal, J. Mater. Sci. Lett. **11**, 496 (1992).
[39] J. F. Moulder, W. F. Stickle, P. E. Sobol, and K. D. Bomben, *Handbook of X-Ray Photoelectron Spectroscopy* (Physical Electronics, Inc., Minnesota, 1995), p. 81 & 153.
[40] R. C. O' Handley, *Modern Magnetic Materials, Principles and Applications* (Wiley, New York, 2000), p.125.
[41] I. I. Yaacob, A. C. Nunes, and A. Bose, J. Colloid Interface Sci. **171**, 73 (1995).
[42] E. E. Carpenter, J. Magn. Magn. Mater. **225**, 17 (2001).
[43] J. A. Dean, *Lange's Handbook of Chemistry*, 14th. edition (McGraw Hill, New York, 1992), p. 3.35.
[44] A. Roch, R. N. Muller, and P. Gillis, J. Chem. Phys. **110**, 5403 (1999).